Supporting Information

Optimized Electron Occupancy of Solid-Solution Transition Metal for Suppressing Oxygen Evolution of Li$_2$MnO$_3$

Erhong Song, [1,a] Yifan Hu,[1,a] Ruguang Ma,[a]* Yining Li, [a] Xiaolin Zhao, [a] Jiacheng Wang, [a] Jianjun Liu,[a,b,c]*

[a] State Key Laboratory of High Performance Ceramics and Superfine Microstructure, Shanghai Institute of Ceramics, Chinese Academy of Sciences, 1295 Dingxi Road, Shanghai 200050, China

[b] Center of Materials Science and Optoelectronics Engineering, University of Chinese Academy of Sciences, Beijing 100049, China

[c] School of Chemistry and Materials Science, Hangzhou Institute for Advanced Study, University of Chinese Academy of Sciences, 1 Sub-lane Xiangshan, Hangzhou 310024, China

[1] These authors contributed equally to this work. All authors have given approval to the final version of the manuscript.

Corresponding mail: jliu@mail.sic.ac.cn; maruguang@mail.sic.ac.cn

Supporting Data
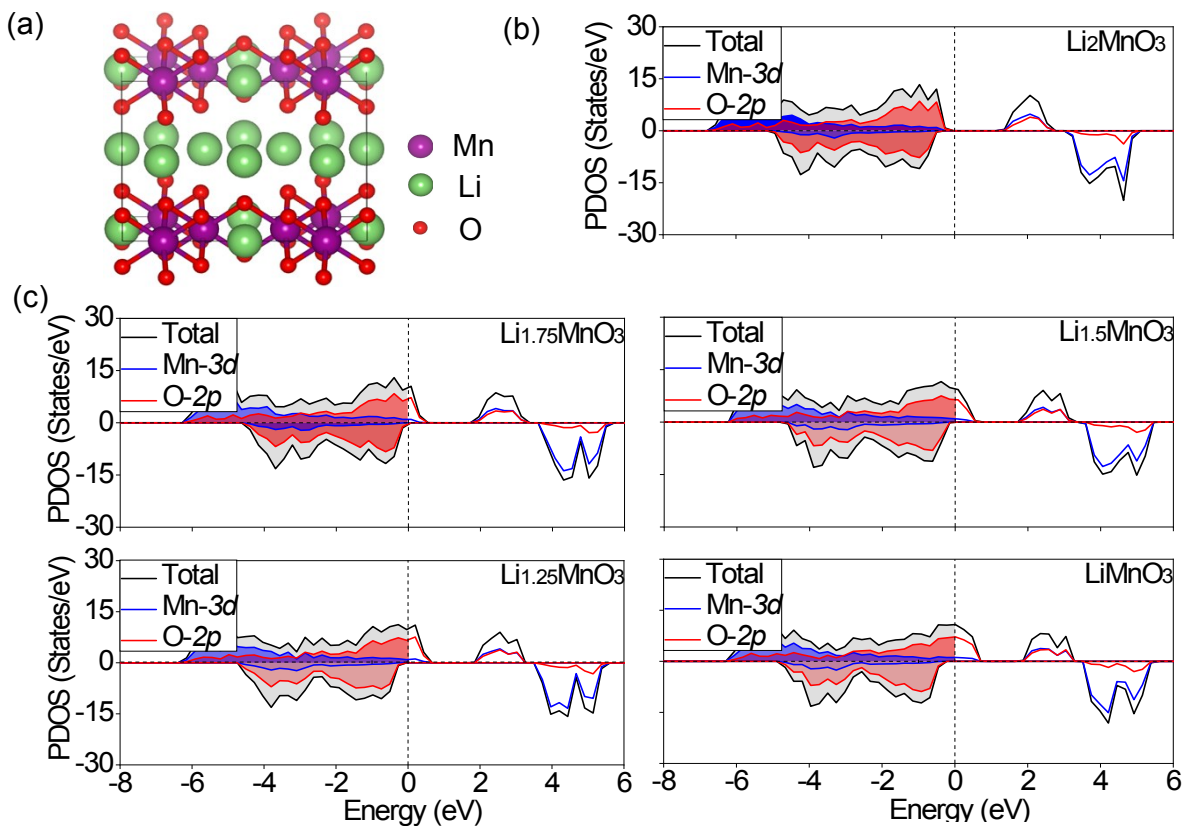
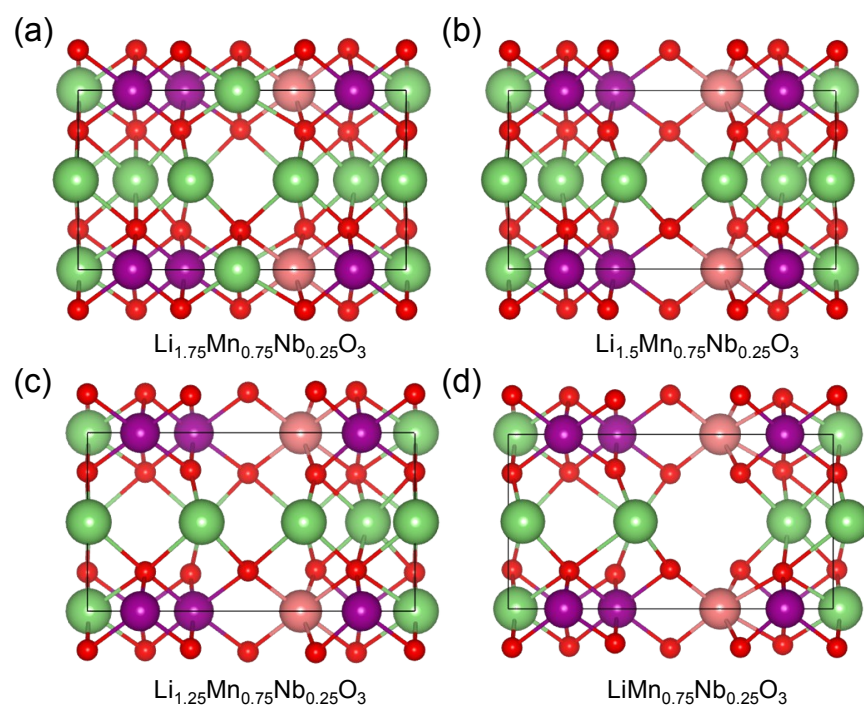**Fig. S1.** Monoclinic (C2/m) and electronic structure of Li-rich layer oxide Li_2MnO_3. (a) Atomic models of the monoclinic Li_2MnO_3 structure. Green spheres are Li, purple spheres are Mn, and small red spheres are O. (b) Density of states of the fully relaxed Li_2MnO_3 for the $3d$-orbital of the Mn ion and the $2p$-orbital of the surrounding O ions. (c) Density of states of the ground state structure of Li_yMnO_3 (y = 1.75, 1.5, 1.25, and 1) determined by the "supercell" software package
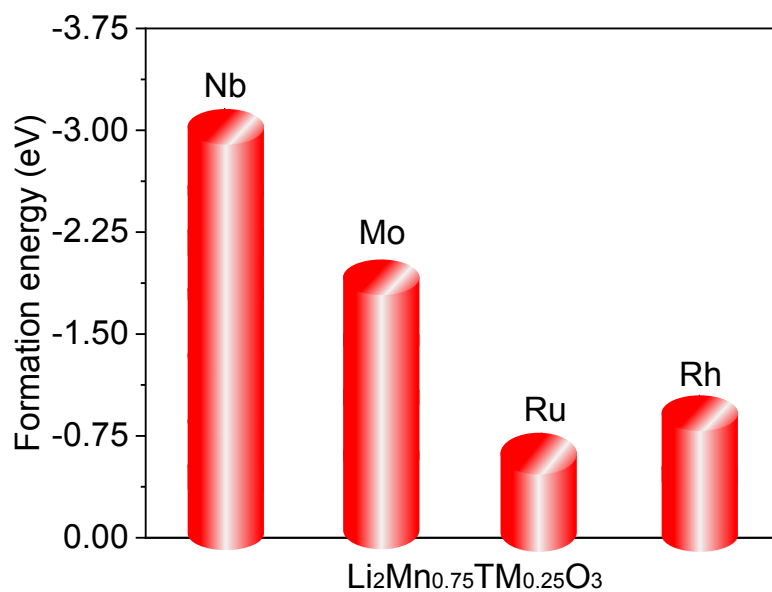
Fig. S2. The formation energies of proposed configurations of $Li_2Mn_{0.75}TM_{0.25}O_3$. The formation energies are calculated as $E_f = E$ ($Li_2Mn_{0.75}TM_{0.25}O_3$) $- E$ ($Li_2Mn_{0.75}\square_{0.25}O_3$) $- 0.25E$ (TM) (TM= Nb, Mo, Ru and Rh, $\square =$ TM vacancy).
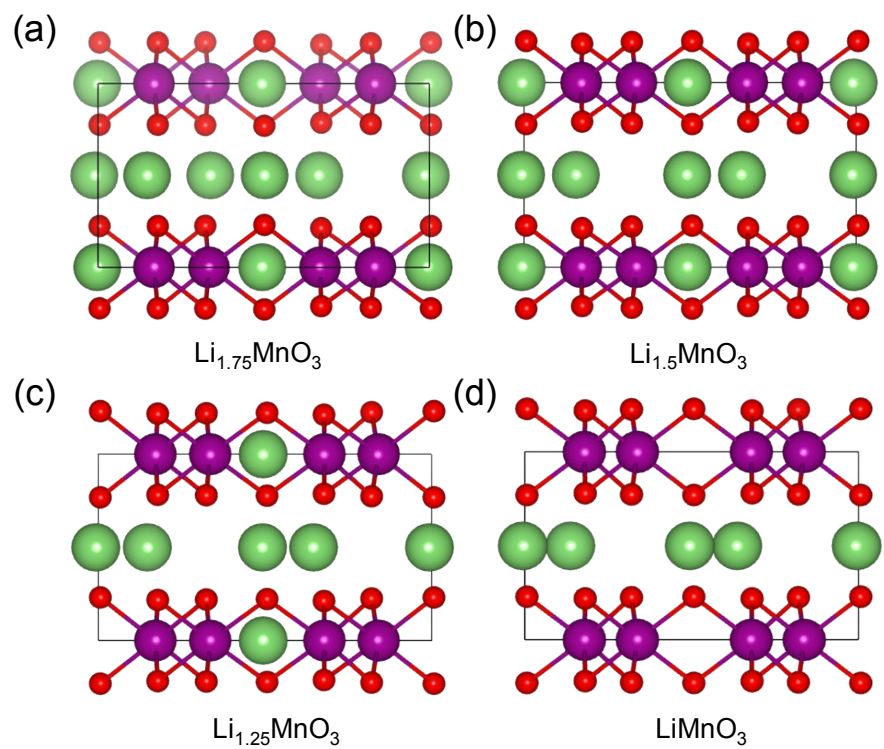
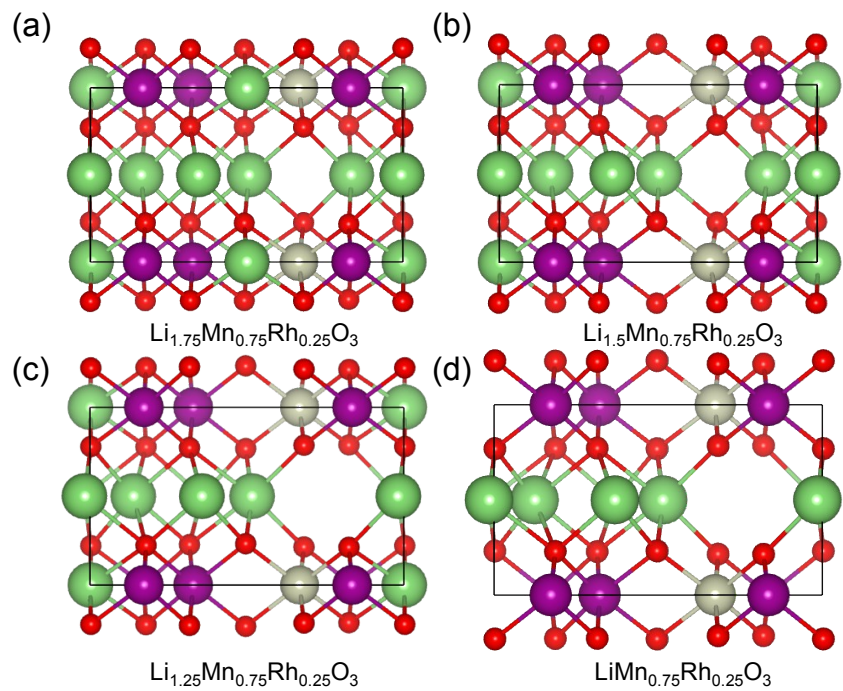(a) Li$_{1.75}$MnO$_3$

(b) Li$_{1.5}$MnO$_3$

(c) Li$_{1.25}$MnO$_3$

(d) LiMnO$_3$

Fig. S3. The optimized structure of Li$_y$MnO$_3$ (y = 1.75, 1.5, 1.25, and 1) determined by the "supercell" software package.

(a) $Li_{1.75}Mn_{0.75}Nb_{0.25}O_3$

(b) $Li_{1.5}Mn_{0.75}Nb_{0.25}O_3$

(c) $Li_{1.25}Mn_{0.75}Nb_{0.25}O_3$

(d) $LiMn_{0.75}Nb_{0.25}O_3$

Fig. S4. The optimized structure of $Li_yMn_{0.75}Nb_{0.25}O_3$ (y = 1.75, 1.5, 1.25, and 1) determined by the "supercell" software package.
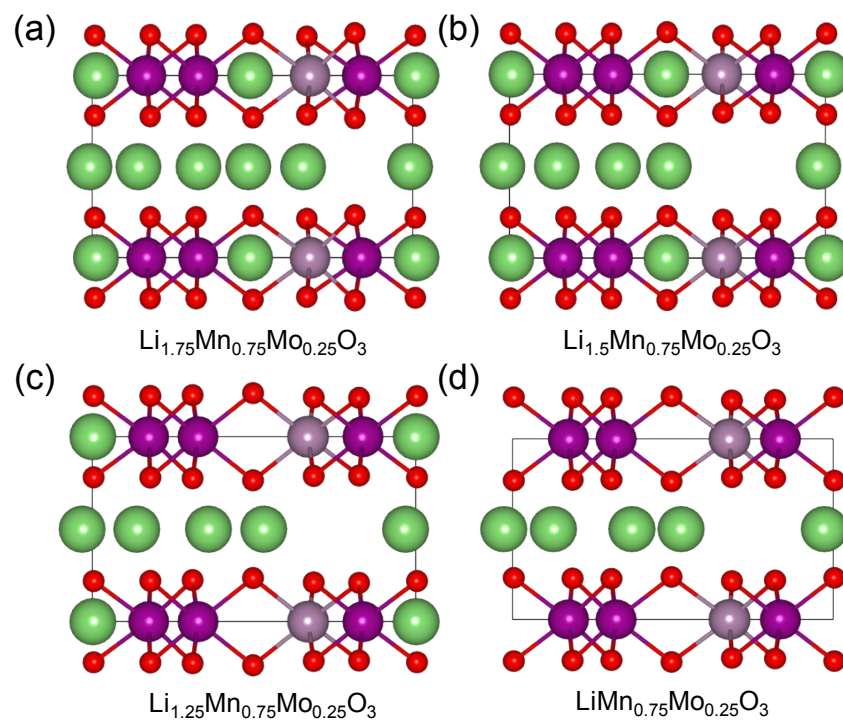
Fig. S5. The optimized structure of $Li_yMn_{0.75}Mo_{0.25}O_3$ (y = 1.75, 1.5, 1.25, and 1) determined by the "supercell" software package.

(a) $Li_{1.75}Mn_{0.75}Rh_{0.25}O_3$
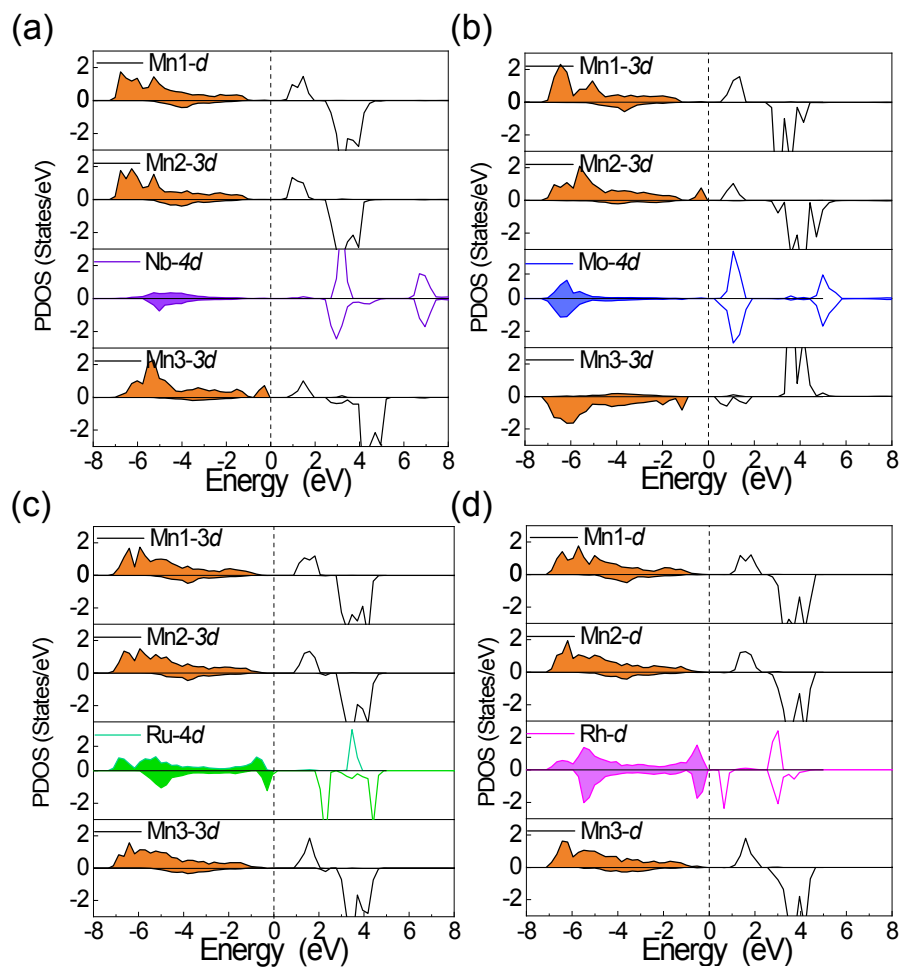
(b) $Li_{1.5}Mn_{0.75}Rh_{0.25}O_3$

(c) $Li_{1.25}Mn_{0.75}Rh_{0.25}O_3$

(d) $LiMn_{0.75}Rh_{0.25}O_3$

Fig. S6. The optimized structure of $Li_yMn_{0.75}Rh_{0.25}O_3$ (y = 1.75, 1.5, 1.25, and 1) determined by the "supercell" software package.
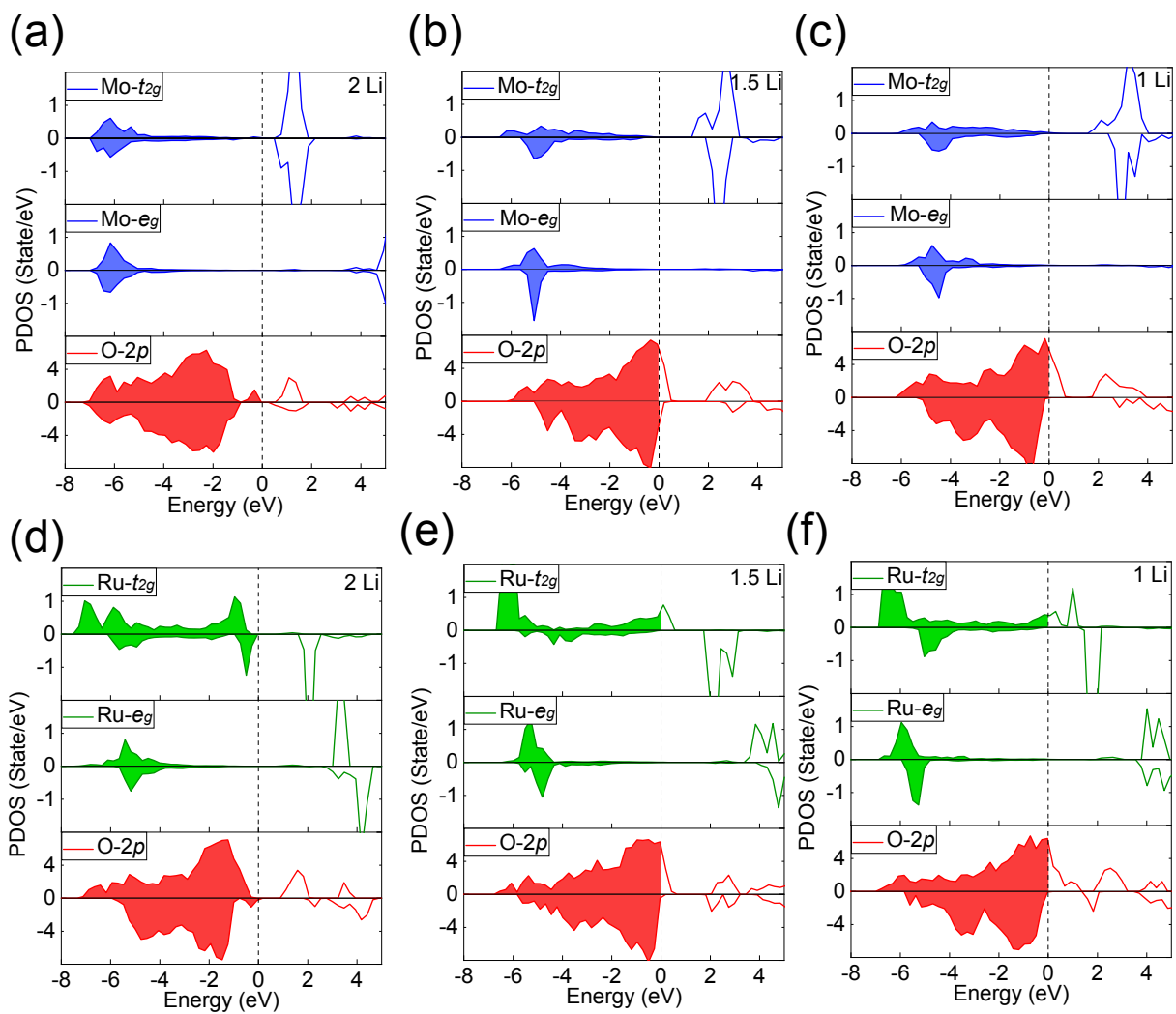
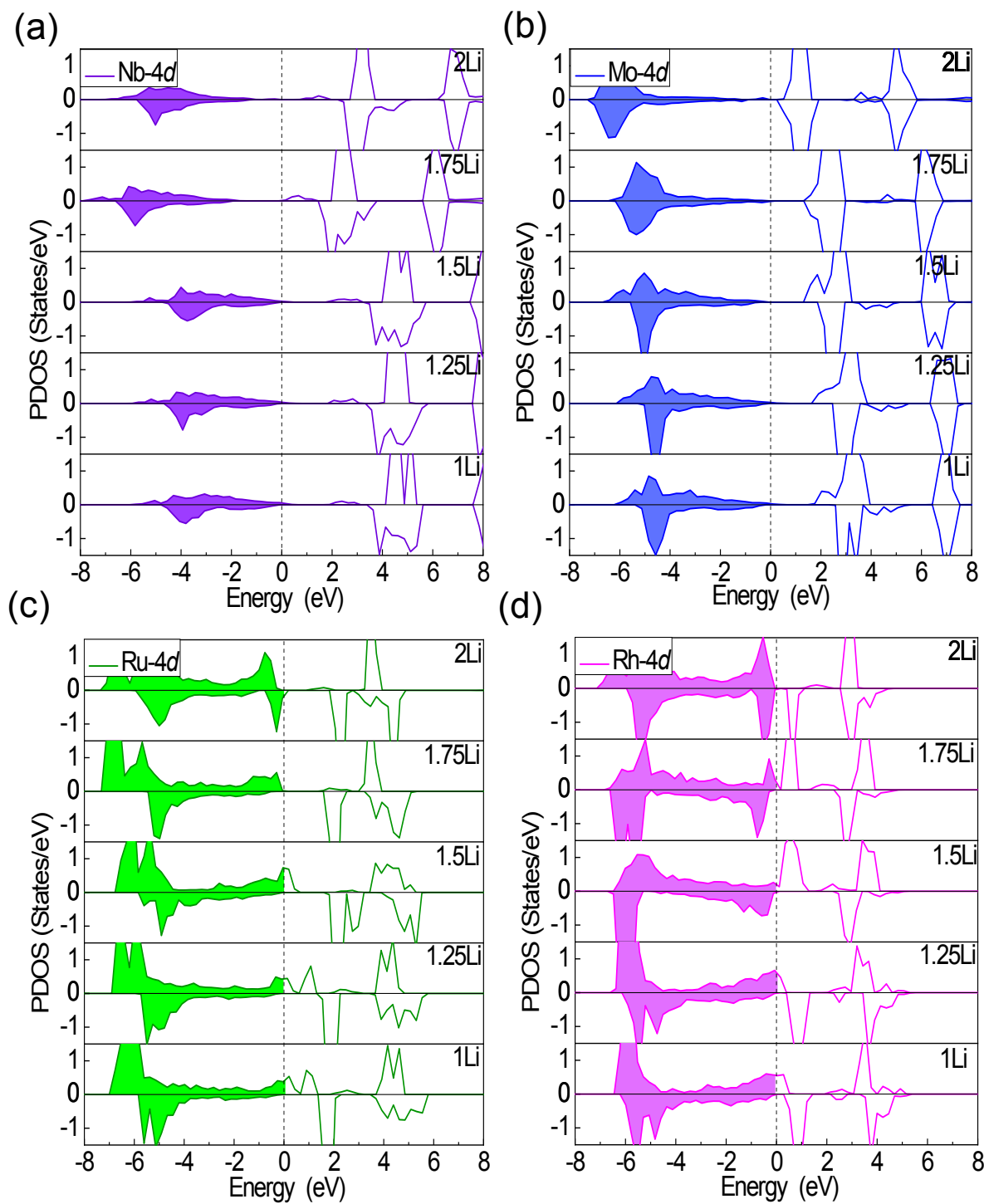**Fig. S7**. Calculated density of states of t_{2g} (d_{xy}, d_{yz}, d_{xz}), e_g (d_{x2-y2}, d_{x2}) of Mo-4d and Ru-4d orbital and O atoms-2p orbital of Li$_y$Mn$_{0.75}$TM$_{0.25}$O$_3$ during the Li extraction (TM= Mo, Ru; y = 2, 1.5 and 1).
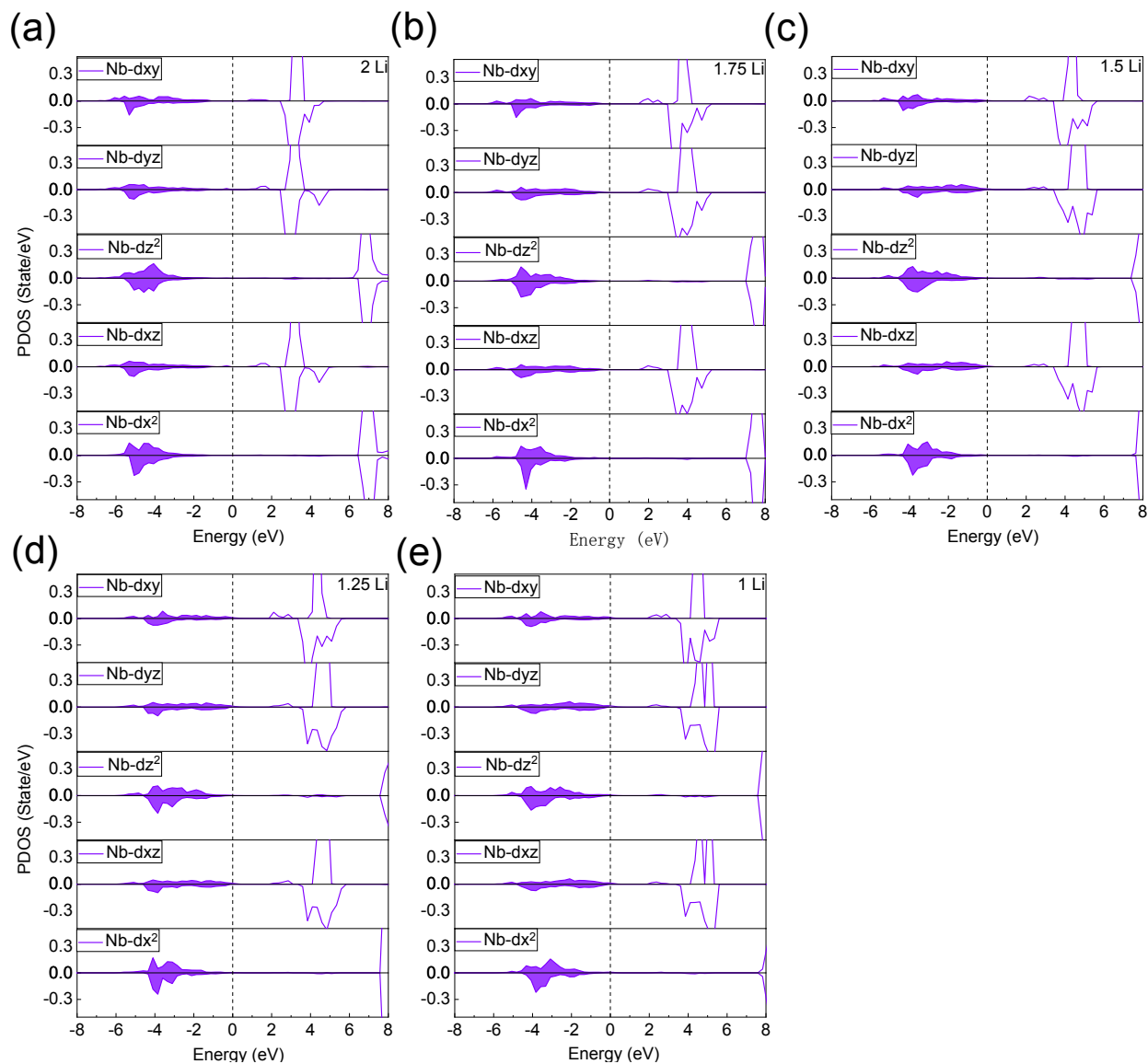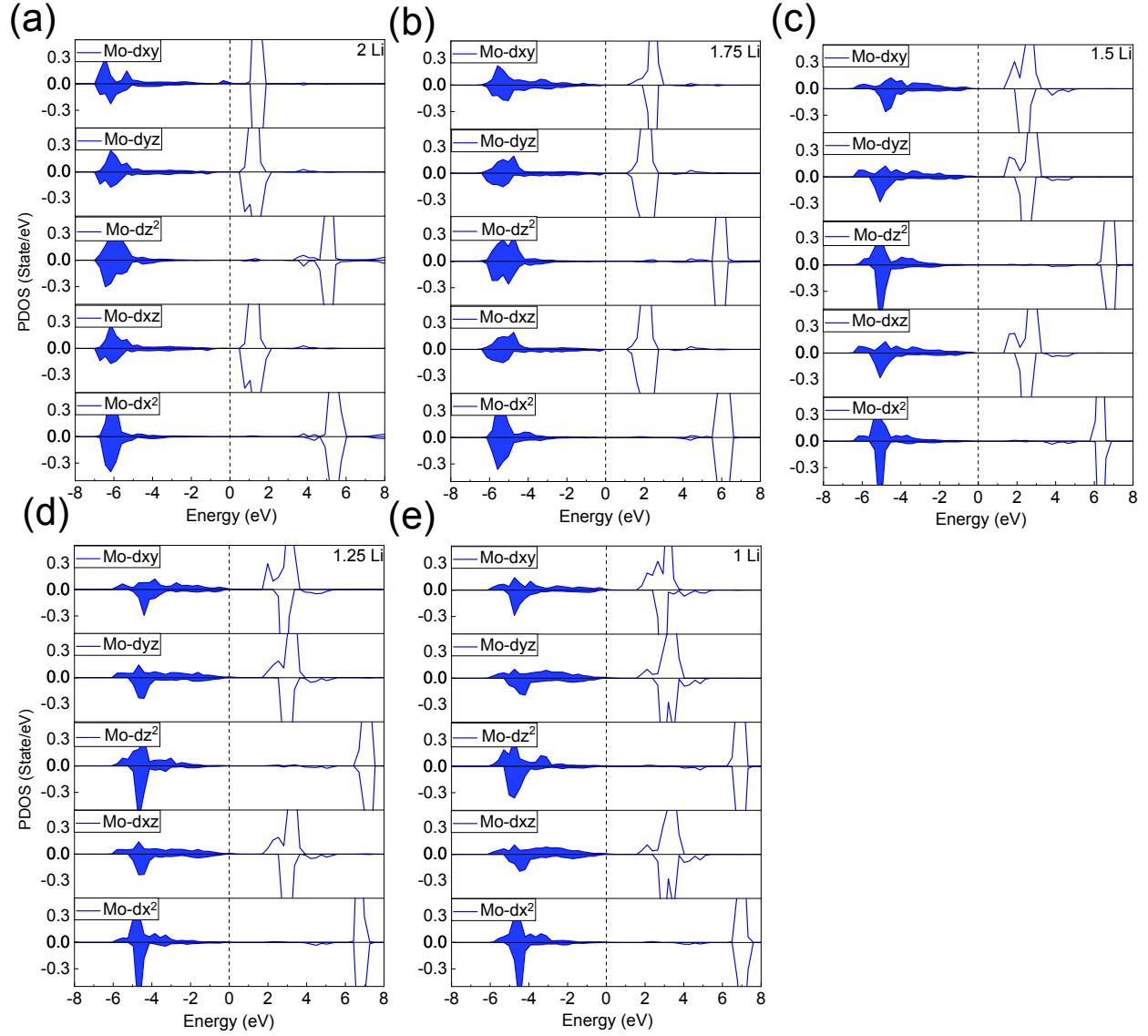
Fig. S8. Calculated projected density of states of the ground state structure of $Li_2Mn_{0.75}TM_{0.25}O_3$ system (TM= Nb, Mo, Ru, Rh).
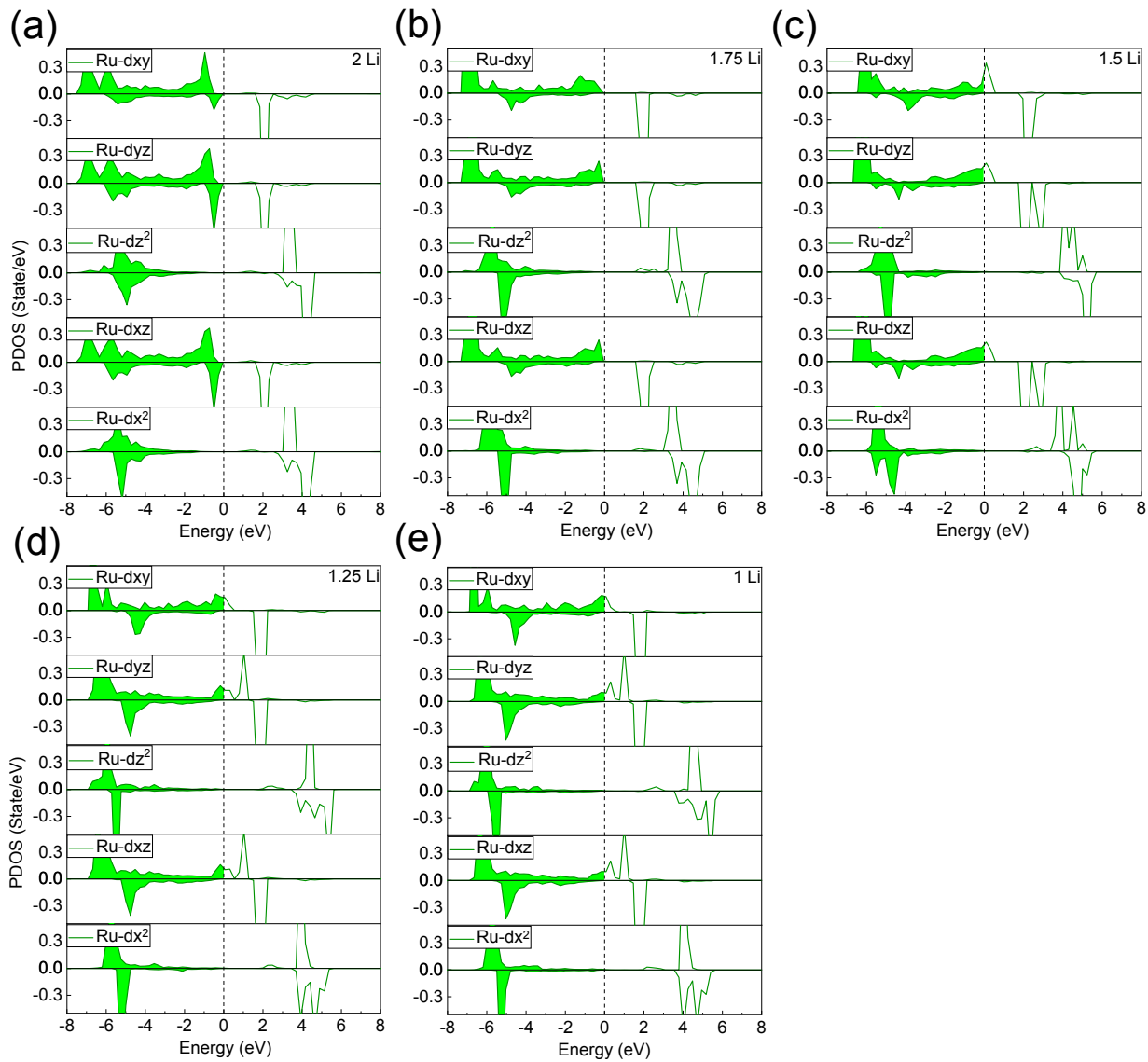
Fig. S9. Calculated projected density of states of the ground state structure of $Li_yMn_{0.75}TM_{0.25}O_3$ system in delithiation process (TM= Nb, Mo, Ru and Rh; y = 2, 1.75, 1.5, 1.25, and 1).

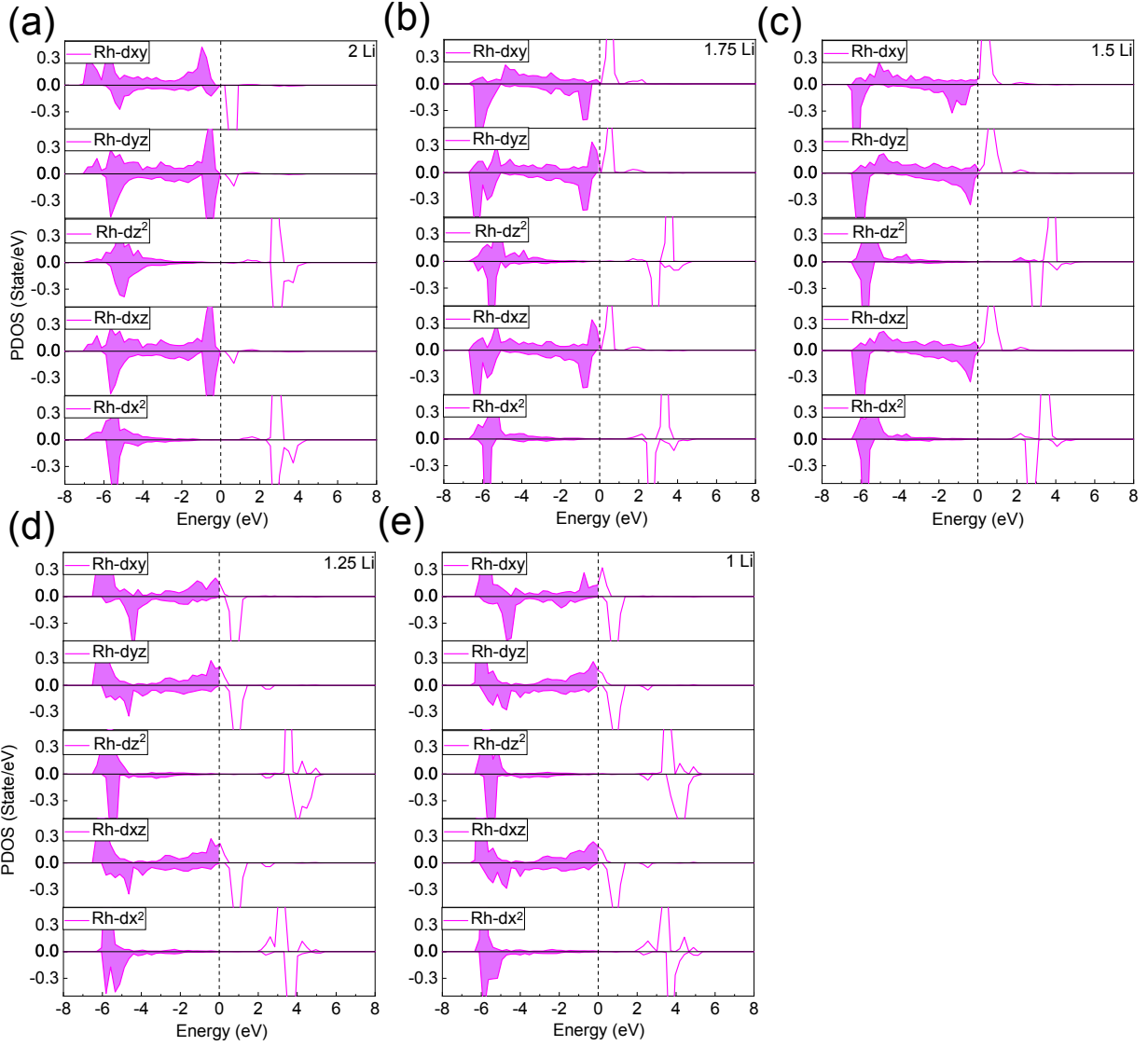**Fig. S10.** Calculated projected density of states of t_{2g} (d_{xy}, d_{yz}, d_{xz}) and e_g (d_{x2-y2}, d_{x2}) of Nb-$4d$ orbital of $Li_yMn_{0.75}Nb_{0.25}O_3$ during the Li extraction (y = 2, 1.75, 1.5, 1.25, and 1).

Fig. S11. Calculated projected density of states of t_{2g} (d_{xy}, d_{yz}, d_{xz}) and e_g (d_{x2-y2}, d_{x2}) of Mo-4d orbital of Li$_y$Mn$_{0.75}$Mo$_{0.25}$O$_3$ during the Li extraction (y = 2, 1.75, 1.5, 1.25, and 1).

Fig. S12. Calculated projected density of states of t_{2g} (d_{xy}, d_{yz}, d_{xz}) and e_g (d_{x2-y2}, d_{x2}) of Ru-4d orbital of Li$_y$Mn$_{0.75}$Ru$_{0.25}$O$_3$ during the Li extraction (y = 2, 1.75, 1.5, 1.25, and 1).

Fig. S13. Calculated projected density of states of t_{2g} (d_{xy}, d_{yz}, d_{xz}) and e_g (d_{x2-y2}, d_{x2}) of Rh-4d orbital of Li$_y$Mn$_{0.75}$Rh$_{0.25}$O$_3$ during the Li extraction (y = 2, 1.75, 1.5, 1.25, and 1).
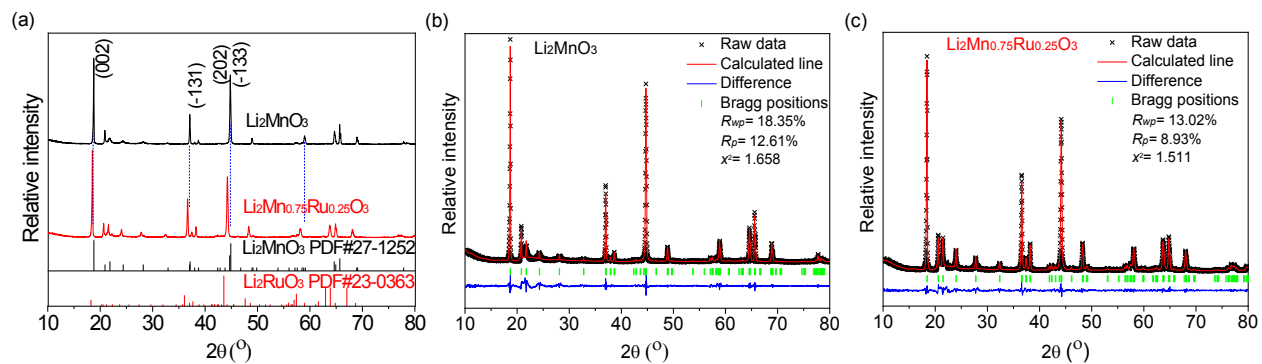
Fig. S14 (a) XRD patterns of Li_2MnO_3 (black line) and $Li_2Mn_{0.75}Ru_{0.25}O_3$ (red line). Rietveld refinement XRD pattern of Li_2MnO_3 (b) and $Li_2Mn_{0.75}Ru_{0.25}O_3$ (c) , respectively.
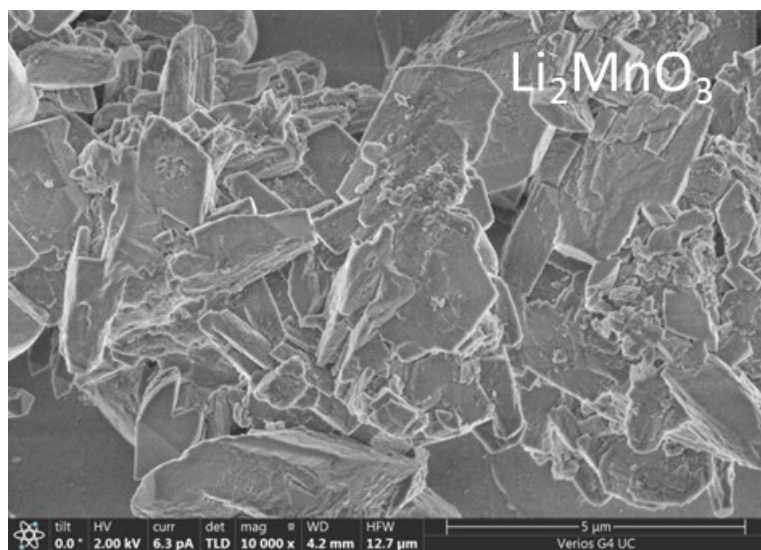
Fig. S15. SEM image of Li$_2$MnO$_3$.
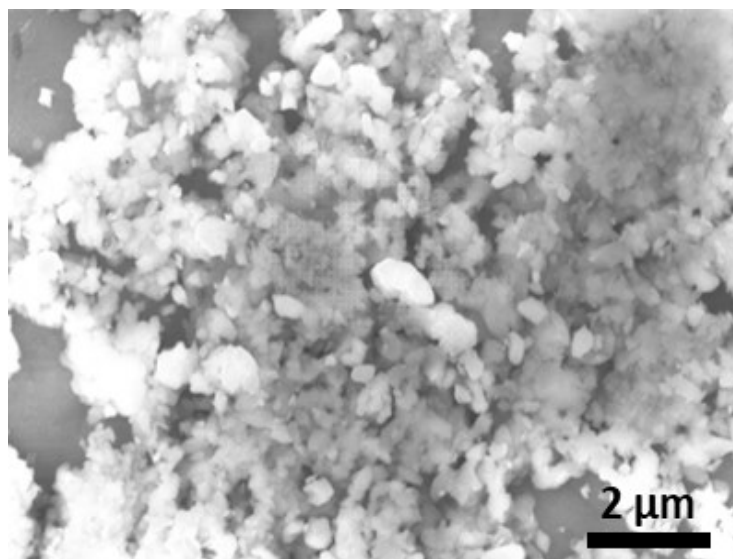
Fig. S16. SEM image of $Li_2Mn_{0.75}Ru_{0.25}O_3$.
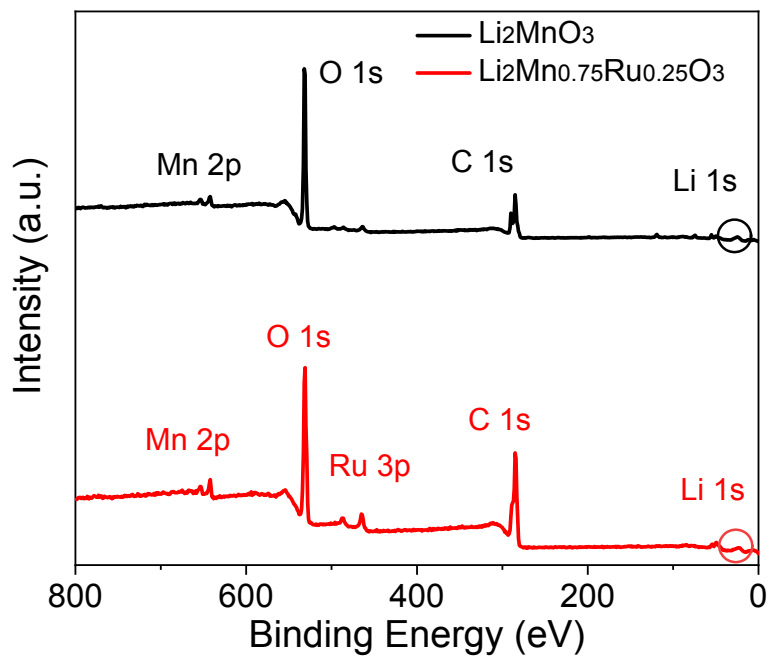
Fig. S17. Survey XPS spectra of Li_2MnO_3 and $Li_2Mn_{0.75}Ru_{0.25}O_3$, respectively.
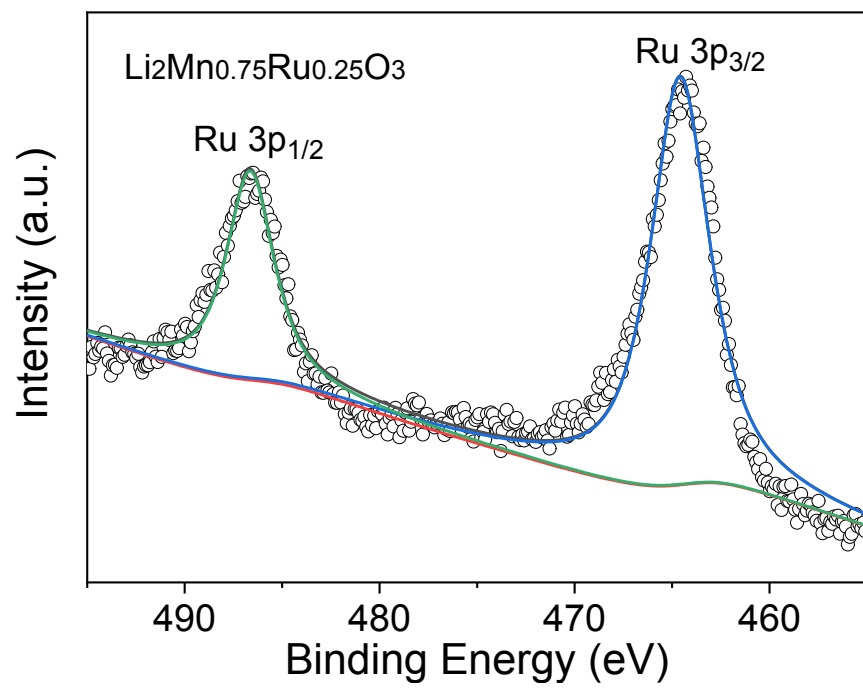
Fig. S18. Survey XPS spectra of $Li_2Mn_{0.75}Ru_{0.25}O_3$.

Table S1 The lattice parameters of Li_2MnO_3 and $Li_2Mn_{0.75}Ru_{0.25}O_3$ compound.

Sample	a	b	c	α	β	γ	V
Li_2MnO_3	4.928	8.530	5.025	90	109.204	90	199.484
$Li_2Mn_{0.75}Ru_{0.25}O_3$	4.982	8.623	5.089	90	109.138	90	206.538